www.czasopisma.pan.pl PAN www.journals.pan.pl
ARCHIVES OF ACOUSTICS
Vol. **40**, No. 1, pp. 117–127 (2015)

DOI: 10.1515/aoa-2015-0014

Effect of Liner Characteristics on the Acoustic Performance of Duct Systems

Chokri OTHMANI[(1)], Taissir HENTATI[(1)], Mohamed TAKTAK[(1)], Tamer ELNADY[(2)], Tahar FAKHFAKH[(1)], Mohamed HADDAR[(1)]

[(1)] *Mechanics, Modeling and Production Research Laboratory*
National School of Engineers of Sfax, University of Sfax
BP. 1173 Sfax 3038, Tunisia

[(2)] *Group for Advanced Research in Dynamic Systems (ASU-GARDS)*
Ain Shams University
1 Elsaryat St., Abbaseya, 11517 Cairo, Egypt; e-mail: mohamed.taktak@fss.rnu.tn

(*received January 27, 2014; accepted September 1, 2014*)

Porous materials are used in many vibro-acoustic applications. Different models describe their performance according to material's intrinsic characteristics. In this paper, an evaluation of the effect of the porous and geometrical parameters of a liner on the acoustic power attenuation of an axisymmetric lined duct was performed using multimodal scattering matrix. The studied liner is composed by a porous material covered by a perforated plate. Empirical and phenomenal models are used to calculate the acoustic impedance of the studied liner. The later is used as an input to evaluate the duct attenuation. By varying the values of each parameter, its influence is observed, discussed and deduced.

Keywords: porous material, perforated plate, duct system, scattering matrix, acoustic attenuation.

1. Introduction

Duct systems are used in buildings, transport vehicles etc. These systems are considered as wave-guides in which sound propagates as presented in (Taktak *et al.*, 2012). To assure the acoustic comfort in these systems, the sound must be reduced to meet the regulations. One of used techniques to achieve this objective is the use of porous materials. These materials are generally characterized by their acoustic impedance, Z, which is a function of porous (the flow resistivity, the tortuosity, the porosity, etc.) and geometric (thickness) parameters. The acoustic impedance is then used to model these materials. It can be used as an input to predict the acoustic propagation and radiation in and from duct systems.

Several models have been proposed to estimate the acoustic impedance of porous materials. The majority of them are semi-empirical models. Zwikker and Kösten (1949) were among the first to develop an empirical model to compute this parameter. Thereafter, other models have been elaborated such as Delany and Bazley (1970), Miki (1990) and Hamet and Berengier (1993). Another approach was proposed by Biot (1956) based on phenomenological models. Later, these models were improved by Johnson *et al.* (1987), Attenborough (1987), Allard (1993) and Lafarge *et al.* (1997) in a way to have more reliability by introducing new acoustic parameters or changing the formulation.

In duct systems, these porous materials are used with a perforated plate to support these materials and allow the penetration of the sound wave into the material. These two components constitute the acoustic liner. The perforated plate is also characterized by its acoustic impedance. Several models exist for modelling the acoustic impedance such as those presented by Hersh and Walker (1977), Guess (1975), Hubbard (1995), Rao and Munjal (1986) and Elnady (2004).

To estimate the acoustic efficiency of the liner, several quantities can be used, e.g. the Insertion Loss (IL) as presented in (Lapka, 2009). The acoustic power attenuation, which presents the ratio between the total acoustical power of incident and transmitted waves, is also an energetic parameter used to evaluate the acoustic efficiency of duct systems. This quantity is computed from the multimodal scattering matrix as presented by Taktak *et al.* (2008; 2010; 2013).

In a previous work (Benjdida *et al.*, 2014), the thermal effect on the acoustic performance of an axisymmetric lined duct with a porous material was studied. This study showed that this parameter has a little influence on the acoustic attenuation of a lined duct. In this paper, the effect of porous and geometric proprieties of a liner composed of a porous material and a perforated plate on the acoustic performance of a duct element is investigated. This investigation is based on the computation of the acoustic power attenuation of a duct using the multimodal scattering matrix computed numerically. By varying the values of these parameters their effects can be studied. The outline of the paper is as follows: in Sec. 2, the multimodal scattering matrix computation method is presented, Sec. 3 presents the estimation of the acoustic impedance of the liner composed by a porous material and a perforated plate, Sec. 4 details the acoustic power attenuation computation, finally, numerical results are presented and discussed in Sec. 5.

2. Multimodal scattering matrix computation

In this section, an overview of the multimodal scattering matrix computation, developed by Taktak *et al.* (2008; 2010; 2013), is presented. This numerical computation was validated by comparison with analytical results of Bi *et al.* (2006) in Taktak *et al.* (2007) and with experience in Taktak *et al.* (2010). The studied case is a rigid-lined-rigid cylindrical duct located between the two axial coordinates z_L and z_R as shown in Fig. 1. The used acoustic liner consists of a perforated plate and absorbing porous material backed by a rigid plate as shown in Fig. 2. This liner can be described by its acoustic impedance Z.

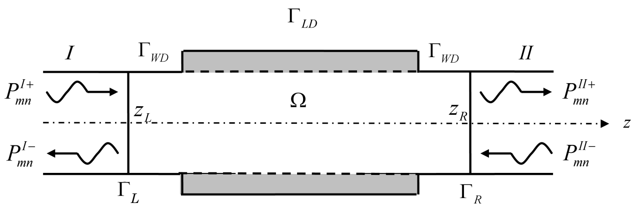

Fig. 1. The calculation domain.

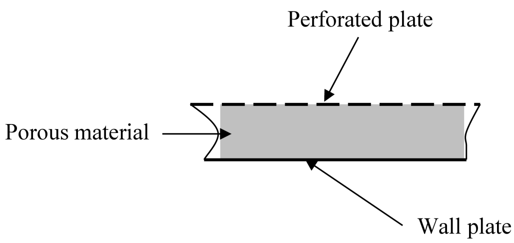

Fig. 2. Composition of the used liner.

The studied duct element is characterized by its multimodal scattering matrix relating the out-coming modal pressure waves array:

$$\mathbf{P}_{2N}^{\text{out}} = \Big\langle P_{00}^{I-}, ..., P_{mn}^{I-}, ..., P_{PQ}^{I-}, \quad P_{00}^{II+}, ..., P_{mn}^{II+} ..., P_{PQ}^{II+} \Big\rangle_N^{\text{T}} \tag{1}$$

to the incoming modal pressure waves array:

$$\mathbf{P}_{2N}^{\text{in}} = \Big\langle P_{00}^{I+}, ..., P_{mn}^{I+}, ..., P_{PQ}^{I+}, \quad P_{00}^{II-}, ..., P_{mn}^{II-}, .., P_{PQ}^{II-} \Big\rangle_N^{\text{T}} \tag{2}$$

as follows

$$\mathbf{P}_{2N}^{\text{out}} = \mathbf{S}_{2N\times 2N}\mathbf{P}_{2N}^{\text{in}} = \begin{bmatrix} \mathbf{R}_{N\times N}^{I} & \mathbf{T}_{I\to II\; N\times N} \\ \mathbf{T}_{II\to I\; N\times N} & \mathbf{R}_{N\times N}^{II} \end{bmatrix}_{2N\times 2N} \mathbf{P}_{2N}^{\text{in}}, \tag{3}$$

where m and n are the circumferential and radial wave numbers respectively, N is the number of propagating modes in both cross sections, P and Q are the circumferential and radial wave numbers respectively associated to the N-th propagating mode ($m \le P$ and $n \le Q$).

$R_{mn,pq}^{I}$ is the reflection coefficient of the wave incident to the element from the side I, $T_{II\to I\; mn,pq}$ is the transmission coefficient of the wave from side II to side I, $R_{mn,pq}^{II}$ is the reflection coefficient of the wave incident to the element from the side II and $T_{I\to II\; mn,pq}$ is the transmission coefficient of the wave from side I to side II.

The acoustical pressure p in the duct is the solution of the following system:

$$\begin{aligned} k^2 p + \Delta p = 0 \quad & \text{for} \quad \Omega, \\ \frac{\partial p}{\partial n_W} = 0 \quad & \text{for} \quad \Gamma_{WD}, \\ Z\frac{\partial p}{\partial n_L} = i\omega\rho p \quad & \text{for} \quad \Gamma_{LD}, \end{aligned} \tag{4}$$

where k is the wave number, Ω is the acoustic domain inside the duct, Γ_{WD} and Γ_{LD} corresponds to the rigid and lined walls respectively, $\mathbf{n}_W$ and $\mathbf{n}_L$ are the normal vectors of these walls, and Z is the normalized acoustic impedance.

To solve the system of Eqs. (4) the Finite Element Method is used. The corresponding weak variational formulation can be written as:

$$\Pi = -\int\limits_{\Omega} (\nabla q \cdot \nabla p)\,\mathrm{d}\Omega + k^2 \int\limits_{\Omega} qp\,\mathrm{d}\Omega + \int\limits_{\cup\Gamma_i} q\frac{\partial p}{\partial n_i}\,\mathrm{d}\Gamma_i = 0, \tag{5}$$

where q is the test function, $\mathrm{d}\Omega$ and $\mathrm{d}\Gamma_i$ are the integration elements through the duct domain and boundaries respectively, and $\cup\Gamma_i$ presents the whole boundary. The last integral of this formulation is given by the following expression by adding the modal incoming and out coming pressures as additional degrees of freedom to the model:

$$\begin{aligned}\int\limits_{\cup\Gamma_i} q\frac{\partial p}{\partial n}\,\mathrm{d}\Gamma &= \int\limits_{\Gamma_t} q\left(\frac{i\omega\rho p}{Z}\right)\,\mathrm{d}\Gamma_{LD}\\ &+\sum_{n}^{N_r} ik_{mn}\left[\left(n_L\left(P_{mn}^{I+}-P_{mn}^{I-}\right)\int\limits_{\Gamma_L} qJ_m\left(\chi_{mn}r\right)\,\mathrm{d}\Gamma_L\right)\right.\\ &\left.+\left(n_R\left(P_{mn}^{II+}-P_{mn}^{II-}\right)\int\limits_{\Gamma_R} qJ_m\left(\chi_{mn}r\right)\,\mathrm{d}\Gamma_R\right)\right],\end{aligned} \tag{6}$$

where J_m is the Bessel function of the first kind of order m. χ_{mn} is the n-th root satisfying the radial hard-wall boundary condition on the wall of the main duct ($J'\left(\chi_{mn}/a\right)=0$) with a is the duct radius; r is the radial coordinate; Γ_L and Γ_R correspond respectively to the left and right boundaries, $\mathbf{n}_L$ and $\mathbf{n}_R$ are their corresponding normal vectors.

For a fixed m, the system (5) results in the following matrix system by taking into account boundary conditions

$$\left\langle\left\langle\, q_1\ \cdots\ q_M\,\right\rangle\ \langle 1\cdots 1\rangle\right\rangle \begin{bmatrix} \mathbf{K} & \mathbf{E}_1 & \mathrm{E}_2 & \mathbf{F}_1 & \mathbf{F}_2\\ \mathbf{G}_1 & \mathbf{G}_2 & \mathbf{G}_3 & \mathbf{0} & \mathbf{0}\\ \mathbf{0} & \mathbf{0} & \mathbf{0} & \mathbf{0} & \mathbf{0}\\ \mathbf{0} & \mathbf{0} & \mathbf{0} & \mathbf{0} & \mathbf{0}\\ \mathbf{H}_1 & \mathbf{0} & \mathbf{0} & \mathbf{H}_2 & \mathbf{H}_3 \end{bmatrix} \cdot \left\{\begin{matrix} \left\{\begin{matrix} p_1\\ \vdots\\ p_M\end{matrix}\right\}\\ \left\{P_{mn}^{I-}\right\}\\ \left\{P_{mn}^{I+}\right\}\\ \left\{P_{mn}^{II-}\right\}\\ \left\{P_{mn}^{II+}\right\}\end{matrix}\right\} = \left\{\begin{matrix}0\\ \vdots\\ \vdots\\ 0\end{matrix}\right\}, \tag{7}$$

where M is the node number in the domain Ω. $\mathbf{K}$ is a matrix relating the test function to the nodal pressures in the domain; $\mathbf{E}_1$, $\mathbf{E}_2$, $\mathbf{F}_1$ and $\mathbf{F}_2$ are matrices relating the test function to the modal pressures on Γ_L and Γ_R; $\mathbf{G}_1$, $\mathbf{G}_2$ and $\mathbf{G}_3$ are matrices relating the nodal acoustic pressures in Ω to different modal pressures on the boundary Γ_L; $\mathbf{H}_1$, $\mathbf{H}_2$ and $\mathbf{H}_3$ are matrices relating the nodal acoustic pressures to different modal pressures on the boundary Γ_R. From this matrix system the multimodal scattering matrix is deduced.

3. Modelling of the liner

It is important to accurately model the acoustic impedance of the liner which is used in the computation of the multimodal scattering matrix. One model for the porous material and another one for the perforated plate are used. The following models are chosen:

1. The Lafarge-Allard model, presented by (Allard, 1993) and (Lafarge *et al.*, 1997), is used to estimate the acoustic impedance for porous materials. This model uses 6 porous parameters (flow resistivity σ, porosity φ, turtousity α_∞, thermal permeability k_0', viscous and thermal characteristic lengths Λ and Λ' to compute the acoustic impedance of the porous material. As mentioned by Sagartzazu and Hervella (2008), the acoustic impedance given by this model is accurate and it is almost similar to those given by other models like Delany-Bazley (1970) and Hamet-Berengier (1993).
2. The Elnady (2004) model is used to estimate the acoustic impedance of the perforated plate. The accuracy of this model was proven by an extensive comparison of its results with those given by several perforated plate impedance models such as Selamet *et al.* (2004). This model was also validated by measurements carried out in Elnady and Boden (2003). This model has been used later by several references (Elnady *et al.*, 2009) and (Elnady *et al.*, 2010) which have proven to be efficient and accurate.

The acoustic impedance of the liner is obtained as follows:

$$Z = Z_{\text{Porous Material}} + Z_{\text{Perforated Plate}} \tag{8}$$

with

$$Z_{\text{Porous Material}} = Z_c\coth(jk_cd_m), \tag{9}$$

where Z_c and k_c are the surface characteristic impedance and propagation constant respectively, and d_m is the material depth. The values of Z_c and k_c are estimated by the Lafarge-Allard model as detailed in the following section.

3.1. *Porous material acoustic impedance model: the Lafarge-Allard model*

This model expresses respectively the dynamic compressibility K_{LA} and the effective density ρ of the fluid saturating the porous medium rigid structure as presented by Allard (1993) and Lafarge *et al.* (1997) as follows:

$$\rho = \alpha_\infty\rho_0\left[1-j\frac{\sigma\varphi}{\rho_0\alpha_\infty\omega}\sqrt{1+\frac{4j\rho_0\alpha_\infty^2\omega\eta}{\sigma^2\varphi^2\Lambda^2}}\right], \tag{10}$$

$$K_{LA} = \gamma P_0\left[\gamma-\frac{(\gamma-1)}{1+\frac{\eta\varphi}{j\omega\rho_0 N_{pr}k_0'}\sqrt{1+\frac{4j\omega\rho_0 N_{pr}k_0'^2}{\eta\varphi^2\Lambda'^2}}}\right]. \tag{11}$$

The characteristic impedance Z_c and the propagation constant k_c are then expressed as follows:

$$Z_c = \sqrt{\rho K_{LA}}, \tag{12}$$

$$k_c = \omega\sqrt{\frac{\rho}{K_{LA}}}, \tag{13}$$

where α_∞ and φ are the material tortuosity and porosity respectively, σ is the material flow resistivity, ρ_0 is the air density, ω is the angular frequency ($\omega = 2\pi f$) with f is the frequency, γ is the ratio of specific heats at respectively constant pressures C_p and volumes C_v defined as follows:

$$\gamma = \frac{C_p}{C_v}. \tag{14}$$

N_{pr} is the Prandtl number, η is the dynamic viscosity, Λ and Λ' are the viscous and thermal characteristic lengths respectively, P is the atmospheric pressure, and k_0' is the thermal permeability.

3.2. Modelling of the perforated plate

The used acoustic impedance model of Elnady (2004) for the perforated plate is expressed as follows

$$\begin{aligned} Z_E = {} & \mathrm{Re}\left\{\frac{ik}{\sigma_p C_D}\left[\frac{t}{F(k_s' d_p/2)} + \frac{\delta_{re}}{F(k_s d_p/2)}\right]\right\} \\ & + i\mathrm{Im}\left\{\frac{ik}{\sigma_p C_D}\left[\frac{t}{F(k_s' d_p/2)} + \frac{\delta_{im}}{F(k_s d_p/2)}\right]\right\}, \end{aligned} \tag{15}$$

where C_D is the discharge coefficient, d_p is the pore diameter, t is the plate thickness, σ_p is plate porosity, δ_{re} and δ_{im} are correction coefficients:

$$\delta_{re} = 0.2 d_p + 200 d_p^2 + 16000 d_p^3, \tag{16}$$

$$\delta_{im} = 0.2856 d_p, \tag{17}$$

$$\begin{aligned} F(k_s d/2) &= 1 - \frac{J_1(k_s d/2)}{k_s \frac{d}{2} J_0(k_s d/2)}, \\ F(k_s' d/2) &= 1 - \frac{J_1(k_s' d/2)}{k_s' \frac{d}{2} J_0(k_s' d/2)}, \end{aligned} \tag{18}$$

$$k_s' = \sqrt{-i\omega/\nu'}, \qquad k_s = \sqrt{-i\omega/\nu}, \tag{19}$$

where ν is the kinematic viscosity and

$$\nu' = 2.179\mu/\rho \tag{20}$$

μ is the dynamic viscosity and ρ is the material density.

4. Acoustical power attenuation

The acoustical power attenuation W_{att} of a duct is the ratio between the total acoustical power of incident waves W^{in} and the total acoustical power of transmitted waves W^{out}. This attenuation is calculated from the scattering matrix as developed by Aurégan and Starobinski (1999):

$$W_{\text{att}} = \frac{W^{\text{in}}}{W^{\text{out}}}. \tag{21}$$

These total energies can be written in the following form:

$$\begin{aligned} W^{\text{in}} &= \mathbf{\Pi}^{\text{in}\,H}_{2N} \cdot \mathbf{\Pi}^{\text{in}}{}_{2N}, \\ W^{\text{out}} &= \mathbf{\Pi}^{\text{out}\,H}_{2N} \cdot \mathbf{\Pi}^{\text{out}}{}_{2N}, \end{aligned} \tag{22}$$

where

$$\begin{aligned} \mathbf{\Pi}^{\text{in}}{}_{2N} &= \mathbf{X}_{2N\times 2N} \cdot \mathbf{P}^{\text{in}}_{2N}, \\ \mathbf{\Pi}^{\text{out}}{}_{2N} &= \mathbf{X}_{2N\times 2N} \cdot \mathbf{P}^{\text{out}}_{2N}, \\ \mathbf{\Pi}^{\text{in T}}{}_{2N} &= \langle \Pi^i_{00}(z_L), ..., \Pi^i_{PQ}(z_L), \\ & \qquad \Pi^{tr}_{00}(z_R), ..., \Pi^{tr}_{PQ}(z_R)\rangle \\ \mathbf{\Pi}^{\text{out T}}{}_{2N} &= \langle \Pi^r_{00}(z_L), ..., \Pi^r_{PQ}(z_L), \\ & \qquad \Pi^t_{00}(z_R), ..., \Pi^t_{PQ}(z_R)\rangle, \end{aligned} \tag{23}$$

$$\mathbf{X}_{2N\times 2N} = \begin{bmatrix} [\mathrm{diag}(X_{mn})]_{N\times N} & 0_{N\times N} \\ 0_{N\times N} & [\mathrm{diag}(X_{mn})]_{N\times N} \end{bmatrix}, \tag{24}$$

$$\Pi^{i,r}_{mn}(z_L) = X_{mn} P^{i,r}_{mn}(z_L),$$

$$\Pi^{t,tr}_{mn}(z_R) = X_{mn} P^{t,tr}_{mn}(z_R),$$

$$X_{mn} = \sqrt{\frac{N_{mn} k_{mn}}{2\rho_0 c_0 k}},$$

where N_{mn} is the normalization factor

$$N_{mn} = S J_m^2(\chi_{mn})\left[1 - \frac{m^2}{\chi_{mn}^2}\right]$$

associated to the mode (mn), $S = \pi a^2$ is the cross-section area, $k_{mn} = \sqrt{k^2 - (\chi_{mn}/a)^2}$ is the axial wave number of mode (m, n) in the main duct χ_{mn} is the n-th root of the first derivate of J_m where J_m is the Bessel function of the first kind of order m. Finally, the acoustical attenuation of the lined duct in dB is written as:

$$W_{\text{att}} = 10\log_{10}\left(\frac{\sum\limits_{i=1}^{2N} |d_i|^2}{\sum\limits_{i=1}^{2N} \lambda_i |d_i|^2}\right), \tag{25}$$

where λ_i are the eigenvalues of the matrix $\mathbf{H}$ and $\mathbf{d}_{2N} = \mathbf{U}^{\text{T}*}_{2N\times 2N}\mathbf{\Pi}^{\text{in}}_{2N}$ with $\mathbf{H}$ is defined as:

$$\mathbf{H}_{2N\times 2N} = \mathbf{S}'^{H}_{2N\times 2N} \cdot \mathbf{S}'_{2N\times 2N}. \tag{26}$$

This matrix can be expressed as:

$$\mathbf{H}_{2N\times 2N} = \mathbf{U}_{2N\times 2N}\mathbf{\Lambda}_{2N\times 2N}\mathbf{U}^{H}_{2N\times 2N}, \tag{27}$$

where $\mathbf{U}$ and $\mathbf{\Lambda}$ are the matrices of eigenvectors and eigen values of $\mathbf{H}$.

5. Numerical results

The studied duct element is a 1 m duct composed of a 0.1 m rigid duct, 0.8 m lined duct and 0.1 m lined duct. The radius of this duct a is 0.075 m. The liner is composed of absorbing porous material and a perforated plate as shown in Fig. 2. The characteristics of the propagation medium (the air), the porous material and the perforated plate are listed in Table 1. The used porous material is the industrial material "*Acusticell*" from Sagartzazu and Hervella (2008). The studied frequency range is ka =[0–3.8] where 3 modes are propagating (ka is the non-dimensional wave number $ka = (2\pi f/c_0).a$).

Figure 3 shows the acoustic power attenuations of the duct versus ka computed using the Delany-Bazley, Hamet-Berengier and Lafarge-Allard porous material

Table 1. The values of the properties of air, porous material and perforated plate used in this work.

Air	c_0	Velocity [m.s^{-1}]	342
	ρ_0	Density [kg.m^{-3}]	1.213
	Z_0	Characteristic impedance [Pa.m^{-1}.s]	414
	γ	Adiabatic constant	1.4
	ka	Normalized wavenumber	$\dfrac{2\pi f a}{c_0}$
	Npr	Prandlt Number	0.708
	P_0	Atmospheric pressure [Pa]	101300
	Nu	Dynamic viscosity [Pa.s]	$1.84 \cdot 10^{-5}$
Acoustic parameter material (Acusticel)	σ	Flow resistivity [N.m^{-1}.s]	22000
	φ	Porosity	0.95
	α_∞	Tortuosity	1.38
	k_0'	Thermal permeability [m^2]	$0.83 \cdot 10^{-8}$
	Λ	Viscous characteristic length [m]	0.00017
	Λ'	Thermal characteristic length [m]	0.00051
	d	Thickness of specimen [m]	0.024
Perforated plate	d_p	Pores diameter [m]	0.001
	σ_p	Plate porosity	2.5%
	t	Plate thickness [m]	0.001
	C_D	Discharge coefficient	0.76

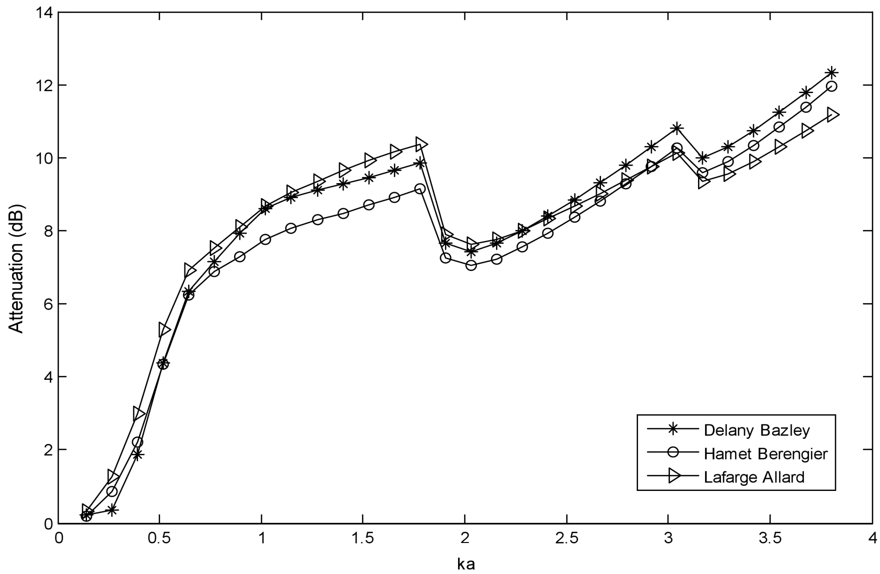

Fig. 3. Acoustic power attenuation of the studied duct for several porous materials models.

models respectively. This Figure shows that the three porous material models give close results and the variation of the attenuation is almost the same for all three models. The difference between these results does not exceed 2 dB. This confirms the conclusion presented in Sagartzazu and Hervella (2008) and shows the similitude in acoustic impedance models for porous materials. The acoustic behavior of the duct element can be described as follows:

The acoustic power attenuation increases when ka increases but there are drops at the mode cut – on frequencies. The maximum of acoustic power attenuation is observed in the final point, the value of this maximum varies for each model (Delany-Bazelay: 12.2 dB, Hamet-Berengier: 12 dB and for Lafarge-Allard: 11.1 dB).

As mentioned in Sec. 3, Lafarge-Allard model is the only model used to estimate the acoustic impedance of porous material for evaluating the effects of the liner characteristics. These effects are studied by varying one of the parameters at a time and leaving the others fixed.

5.1. *Plate characteristics effects*

5.1.1. *Effect of the diameter of the perforated plate*

Figure 4 shows the effect of the diameter of the perforated plate on the acoustic power attenuation when varying this parameter from 0.1 mm to 10 mm. This Figure demonstrates that this parameter has an important effect. It is observed that the attenuation shows a peak with a maximum attenuation for perforation diameters 10 mm, 5 mm and 1 mm. The form of the attenuation curves changes when the perforation diameter is equal to 0.1 mm. Figure 4 shows that when the perforation diameter decreases, the acoustic power attenuation increases. The maximum attenuation changes from 9.1 dB for $d = 10$ mm to 11 dB for $d = 5$ mm and to 16.3 dB for $d = 1$ mm. Moreover, it is observed that the frequency of this maximum increases when the perforation diameter decreases. It changes from $ka = 0.6$ for $d = 10$ mm to $ka = 1$ for $d = 5$ mm and to $ka = 1.8$ for $d = 1$ mm.

5.1.2. *Effect of the porosity of the perforated plate*

Figure 5 shows the effect of the porosity of the perforated plate on the acoustic power attenuation when varying this parameter from 0.1% to 100%. Moreover, this Figure shows that this parameter is influent. By increasing the plate porosity, the acoustic power attenuation curve form changes and its value increases. The acoustic power attenuation presents a peak that the maximum and the corresponding frequency increase when the plate porosity increases ($ka = 0.3$ and $W_{att\ \max} = 9.8$ dB for $\sigma_t = 0.1\%$, $ka = 1$ and $W_{att\ \max} = 14.5$ dB for $\sigma_t = 1\%$, $ka = 2.9$ and $W_{att\ \max} = 17$ dB for $\sigma t = 5\%$, $ka = 3.8$ and $W_{att\ \max} = 18$ dB for $\sigma_t = 10\%$). The acoustic behavior of the liner changes for $\sigma_t = 100\%$ which represents a liner without perforated plate.

5.1.3. *Effect of the thickness of the perforated plate*

Figure 6 presents the effect of the thickness of the perforated plate on the acoustic power attenuation when varying this parameter from 0.5 mm to 8 mm. The decrease of the plate thickness generates an increase of the acoustic power attenuation and the shift of the maximum of attenuation to higher frequencies ($ka = 0.5$ for $t = 8$ mm, $ka = 1.05$ for $t = 4$ mm, $ka = 1.4$ for $t = 2$ mm, $ka = 1.8$ for $t = 1$ mm and 2.4 for $t = 0.5$ mm). For $t \leq 0.5$ mm the peak of at-

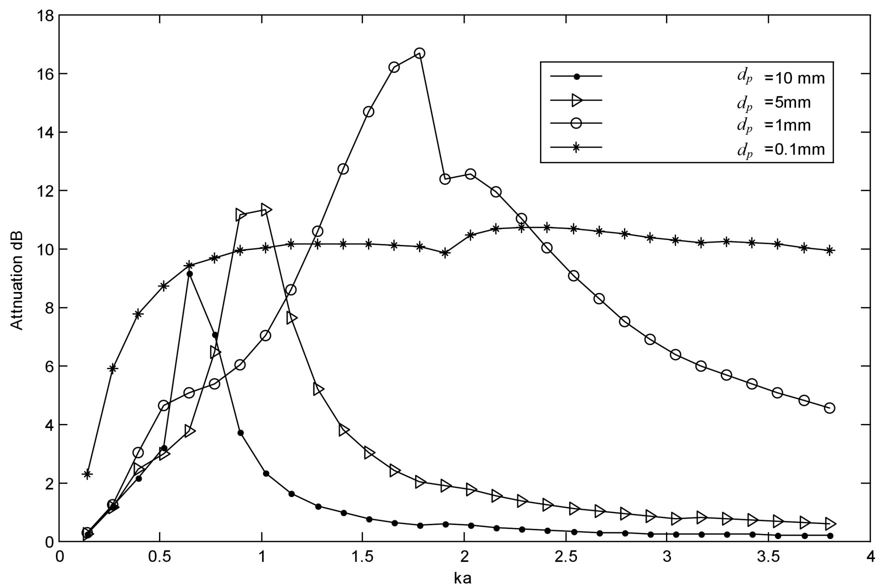

Fig. 4. Effect of the diameter d_p [mm] of the perforated plate on the acoustic power attenuation of the lined duct element.

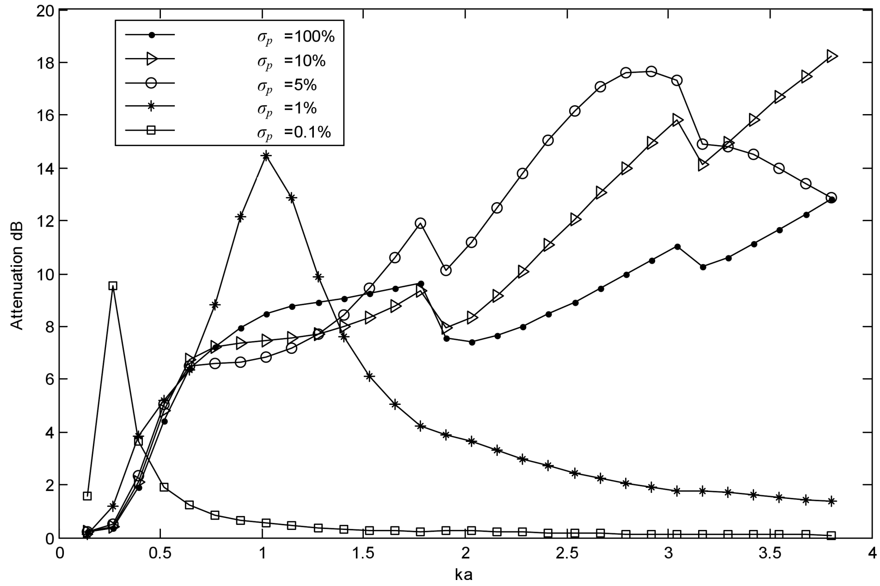

Fig. 5. Effect of the porosity σ_p [%] of the perforated plate on the acoustic power attenuation of the lined duct element.

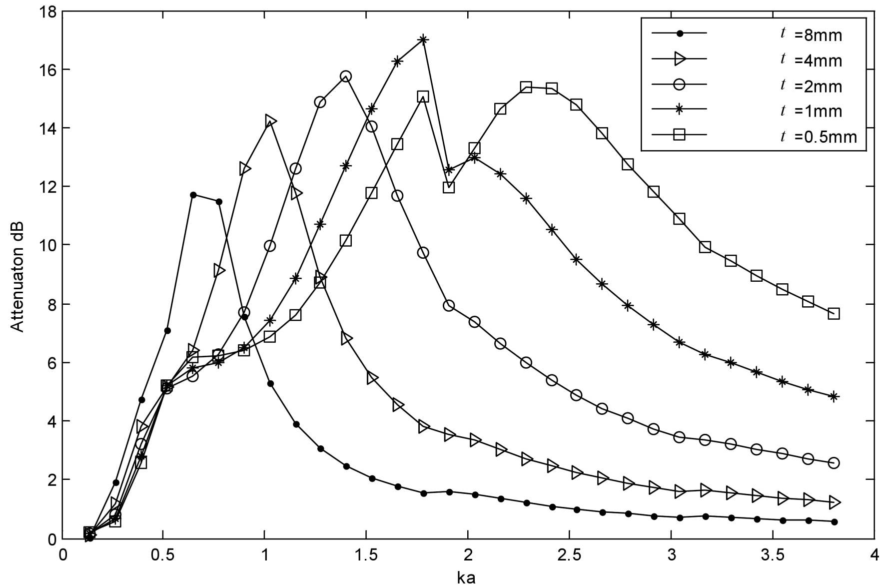

Fig. 6. Effect of the thickness t [mm] of the perforated plate on the acoustic power attenuation of the lined duct element.

tenuation decreases. This Figure shows that the plate thickness is an influent parameter.

5.2. Material proprieties effects

5.2.1. Effect of the flow resistivity of the porous material

Figure 7 presents the effect of the flow resistivity on the acoustic power attenuation. The effect of this parameter is evaluated by varying its value from 1000 $\mathrm{N.m^{-1}.s}$ to 100000 $\mathrm{N.m^{-1}.s}$. The figure shows that the flow resistivity effect is important. It is observed that the variation of the flow resistivity does not influence only on the shape of the curve but also the amplitude of the acoustic attenuation which increases with the increase of the flow resistivity. The maximum of attenuation passes from 14.2 dB for $\sigma_p = 1000\ \mathrm{N.m^{-1}.s}$ to 18.8 dB for $\sigma_p = 10000\ \mathrm{N.m^{-1}.s}$. The increase of the acoustic power attenuation is explained by the increase of the thermal and viscous dissipation into the material when the flow resistivity of the material increases.

5.2.2. Effect of the depth of the porous material

Figure 8 shows the effect of the depth of the porous material on the acoustic power attenuation by varying

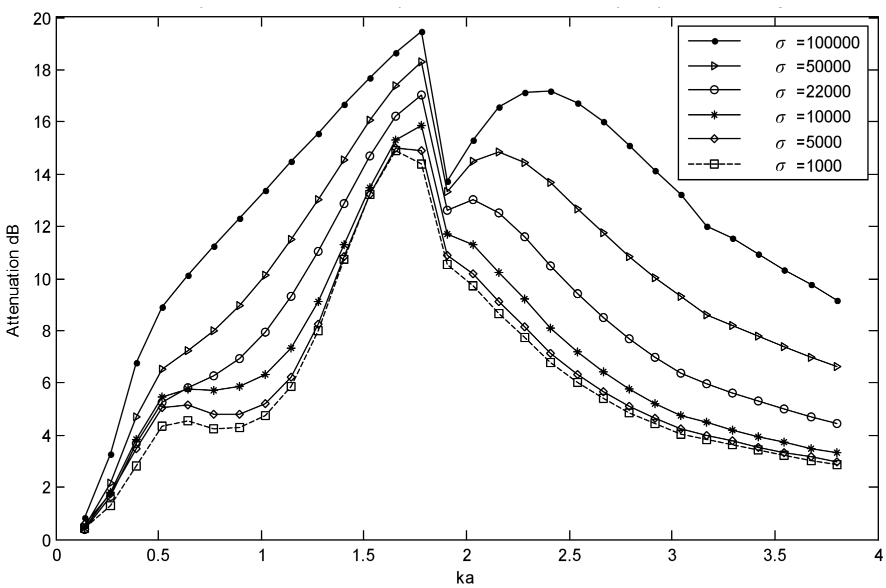

Fig. 7. Effect of the flow resistivity σ [$\mathrm{Nm^{-1}s}$] of the porous material on the acoustic power attenuation of the lined duct element.

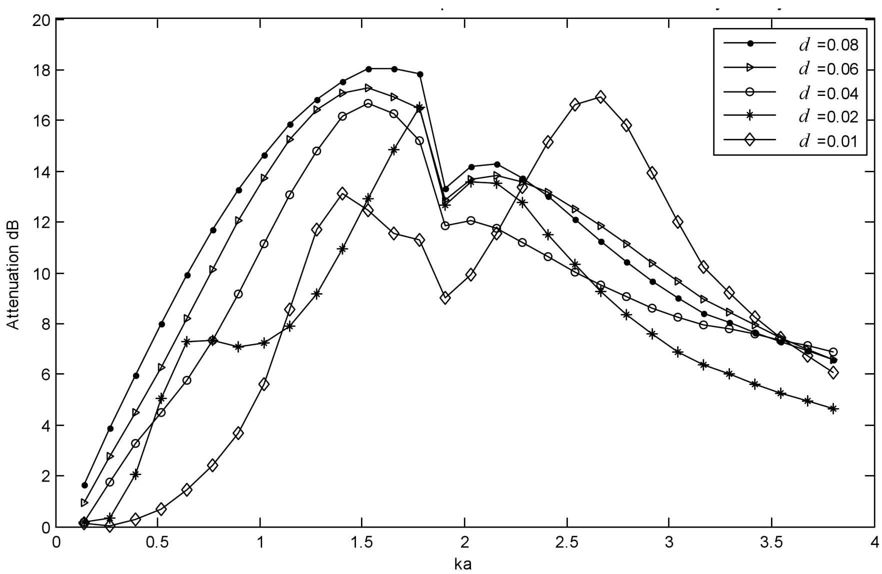

Fig. 8. Effect of the depth d [mm] of the porous material on the acoustic power attenuation of the lined duct element.

this parameter from 0.01 m to 0.08 m. This parameter is also influent and an increase of the thickness of the material sample generates an increase of the acoustic power attenuation (16.5 dB for $d = 0.01$ m to 18 dB for $d = 0.08$ m). Moreover, a shift of the maximum of attenuation frequency is observed: there is a decrease of this frequency when the material depth increases from $ka = 2.6$ for $d = 0.01$ m to $ka = 1.5$ for $d = 0.08$ m. The observed effect is explicated by the augmentation of the material volume that means the increase of contact surface between the acoustic wave and the material structure which increases the dissipation phenomena into the material.

5.2.3. Effect of the porosity and tortuosity of the porous material

Figure 9 shows the effect of the porosity of the porous material on the acoustic power attenuation when varying the material porosity from 0.5 to 0.99. The Lafarge-Allard model predicts the increase of the acoustic power attenuation when this parameter increases. But it is observed that the variation of the acoustic power attenuation is not important and does not exceed 1 dB which permits to conclude that this parameter is not important compared with previous studied parameters. The porosity expresses the fluid

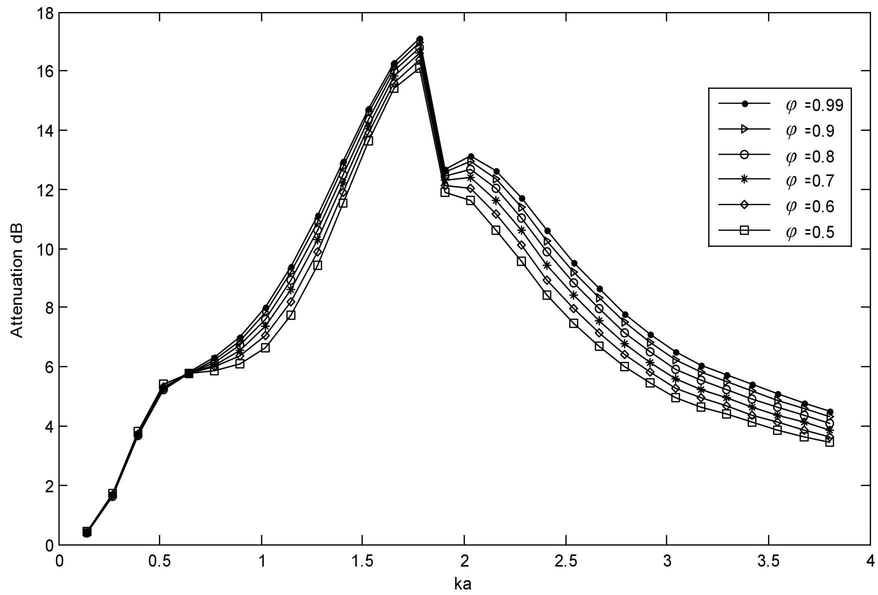

Fig. 9. Effect of the porosity φ of the porous material on the acoustic power attenuation of the lined duct element.

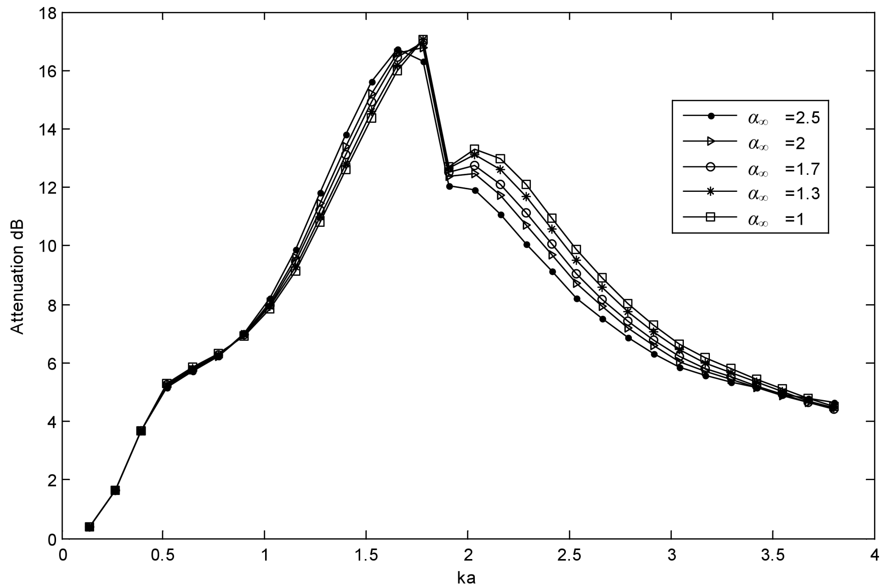

Fig. 10. Effect of the tortuosity σ_∞ of the porous material on the acoustic power attenuation of the lined duct element.

volume. The increase of this parameter generates the increase of the air portion in the material and therefore the dissipation phenomena in the porous material. Figure 10 shows the effect of the tortuosity when varying from 1.3 to 2. Similar to the porosity, the effect of this parameter on the acoustic power attenuation is negligible with small variation.

5.2.4. Effect of the thermal permeability of the porous material

Figure 11 shows the effect of the thermal permeability of the porous material effect on the acoustic power attenuation when varying from 10^{-10} m^2 to 10^{-7} m^2. For this parameter, there is no significant effect caused by this parameter only for the case of $k = 10^{-7}$, especially in the high frequency range.

5.2.5. Effect of the characteristics lengths of the porous material

Figure 12 shows the effect of viscous characteristic length (L_{CV}). When the value of this parameter decreases the acoustic power attenuation decreases except for $L_{CV} = 10^{-5}$ m which presents the maximum of attenuation for a major part of curve. This param-

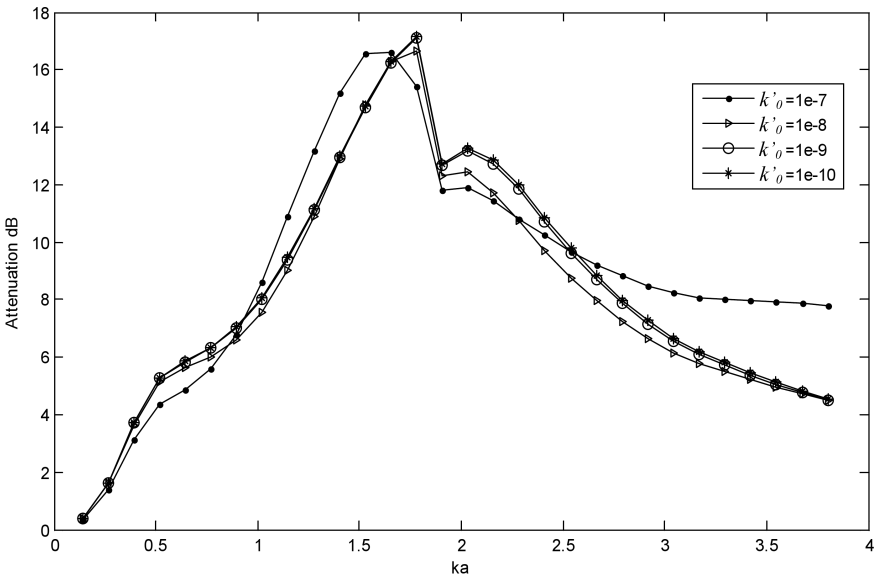

Fig. 11. Effect of the thermal permeability k'_0 [m^2] of the porous material on the acoustic power attenuation of the lined duct element.

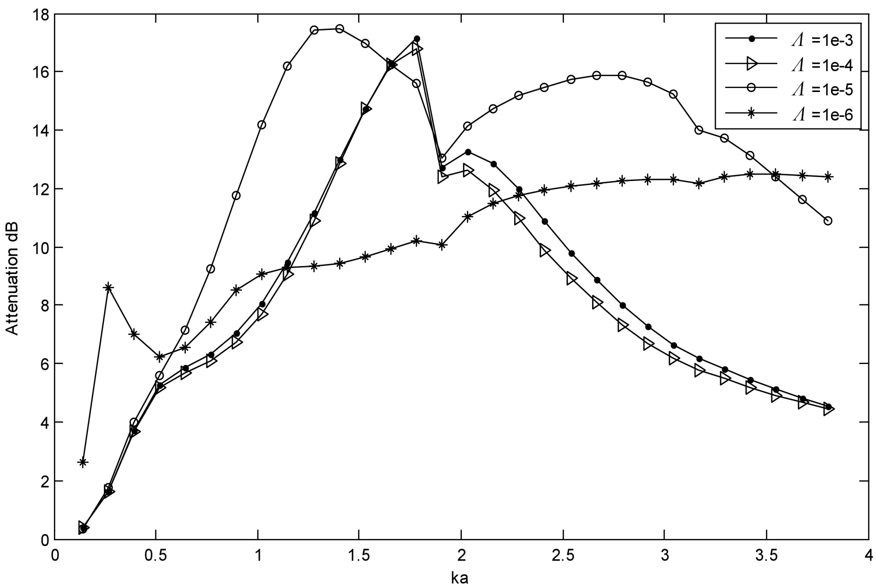

Fig. 12. Effect of the characteristic viscous length Λ [m] of the porous material on the acoustic power attenuation of the lined duct element.

eter does not have an important effect on the acoustic power attenuation only for low values. This figure includes the effect of the thermal characteristic length (L_{CT}) because $L_{CV} = 3.L_{CT}$.

6. Conclusion

The effects of porous and geometric parameters of a liner composed of a porous material and a perforate plate are evaluated. This evaluation is based on the computation of the acoustic power attenuation deduced from the multimodal scattering matrix. The liner is characterized by a model for the perforated sheet and one for the porous material. The objective of this work is to identify the influent liner parameters. To achieve this, a parametric study was applied to a duct element. This study showed that the plate parameters have an important influence on the attenuation. Some porous material characteristics have also an important influence such as the porous material flow resistance and depth. There are also no influent parameters like porous material porosity, tortuosity and permeability and characteristics lengths These parameters must be taken into account in the design and manufacturing of the liner to get the optimum acoustic behavior and attenuate the acoustic wave in ducts systems

Acknowledgments

This work was carried out within the Framework of the Tunisian-Egyptian research project: "Acoustical characterization of acoustic liner materials from agriculture wastes", contract #: 53/4/10, co-funded by the Ministries of Scientific Research in both countries.

References

1. Allard J.F. (1993), *Propagation of sound in porous media: Modeling sound absorbing materials*, Elsevier Applied Science, London 1993, 105–115.
2. Attenborough K. (1987), *On the acoustic slow wave in air-filled granular media*, Journal of Acoustical Society of America, **81**, 93–102.
3. Aurégan Y., Starobinski R. (1999), *Determination of Acoustical energy attenuation/production potentiality from the acoustical transfer functions of a multiport*, Acustica united with Acta Acustica, **85**, 788–792.
4. Benjedidia M., Akrout A., Taktak M., Hammami L., Haddar M. (2014), *Thermal effect on the acoustic behavior of an axisymmetric lined duct*, Applied Acoustics, **86**, 138–145.
5. Bi W.P., Pagneux V., Lafarge D., Aurégan Y. (2006), *Modelling of sound propagation in a non-uniform lined duct using a Multi-Modal Propagation Method*, Journal of Sound and Vibration, **289**, 1091–1111.
6. Biot M. (1956), *Theory of propagation of elastic waves in a fluid-saturated porous solid*, Journal of Acoustical Society of America, **28**, 2, 168–178.
7. Delany M.E, Bazley E.N. (1970), *Acoustical properties of fibrous absorbent materials*, Applied Acoustics, **3**, 105–116.
8. Elnady T. (2004), *Modelling and Characterization of Perforates in Lined Ducts and Mufflers (Paper III)*, Ph.D. Thesis, The Royal Institute of Technology (KTH), Stockholm, Sweden, 2004.
9. Elnady T., Boden H. (2003), *On semi-empirical liner impedance modeling with grazing flow*, Proceedings of 9th AIAA/CEAS, 2003.
10. Elnady T., Elsaadany S., Åbom M. (2009), *Investigation into Modeling of Multi-Perforated Mufflers*, 16th International Congress on Sound and Vibration, Krakow, Poland, July 6–9.
11. Elnady T., Åbom M., Allam S. (2010), *Modeling Perforated Tubes in Mufflers using Two-ports*, ASME Journal of Vibration and Acoustics, **132**, 6.
12. Guess A.W. (1975), *Calculation of perforated plate liner parameters from specified acoustic resistance and reactance*, Journal of Sound and Vibration, **40**, 1, 119–137.
13. Hamet J.F., Bérengier M. (1993), *Acoustical characteristics of porous pavements: a new phenomenological model*, Proceedings Inter-Noise, 1993.
14. Hersh A.S., Walker B. (1977), *Fluid mechanical model of the helmohltz resonator*, Nasa report CR – 2904, 1977.
15. Hubbard H.H. (1995), *Aeroacoustics of Flight Vehicles: Theory and Practice*, 1995.
16. Johnson D.L, Koplik J., Dashen R. (1987), *Theory of dynamic permeability and tortuosity in fluid-saturated porous media*, Journal of Fluid Mechanics, **176**, 379–402.
17. Lafarge D., Lemarinier P., Allard J.F. (1997), *Dynamic compressibility of air in porous structures at audible frequencies*, Journal of Acoustical Society of America, **102**, 4, 1995–2006.
18. Lapka W. (2009), *Insertion Loss of Spiral Ducts – Measurements and Computations*, Archives of Acoustics, **34**, 4, 537–545.
19. Miki Y. (1990), *Acoustical properties of porous materials – Modifications of Delany-Bazley models*, Journal of the Acoustica Society of Japan, 19–24.
20. Rao K.N., Munjal M.L. (1986), *Experimental evaluation of impedance of perforates with grazing flow*, Journal of Sound and Vibration, **108**, 283–295.
21. Sagartzazu X., Hervella L. (2008), *Review in Sound Absorbing Materials*, Archives of Computational Methods in Engineering, **15**, 3, 311–342.
22. Selamet A., Zu M.B., Lee I.J., Huff N.T. (2004), *Analytical approach for sound attenuation in perforated dissipative silencers*, Journal of the Acoustical Society of America, **115**, 2091–2099.
23. Taktak M., Ville J.M., Haddar M., Foucart F. (2007), *Détermination de l'impédance acoustique de matériau par mesure de la matrice de diffusion multimodale*, Proceedings of CMSM 2007.
24. Taktak M., Ville J.M., Haddar M., Foucart F. (2008), *Evaluation of a lined duct performance based on a 3D two port scattering matrix*, Proceedings of Meetings in Acoustics, **4**, 1–14.
25. Taktak M., Ville J.M., Haddar M., Gabard G., Foucart F. (2010), *A indirect method for the characterization of locally reacting liners*, Journal of Acoustical Society of America, **127**, 6, 3548–3559.
26. Taktak M., Majdoub M.A., Ben Tahar M., Haddar M. (2012), *Numerical Modelling of the Acoustic Pressure Inside an Axisymmetric Lined Flow Duct*, Archives of Acoustics, **37**, 2, 151–160.
27. Taktak M., Majdoub M.A., Ben Tahar M., Haddar M. (2013), *Numerical Characterization of Axisymmetric Lined Duct with Flow using Multimodal Scattering matrix*, Journal of Theoretical and Applied Mechanics, **51**, 2, 313–325.
28. Zwikker C., Kosten C.W. (1949), *Sound absorbing materials*, Elsevier edition, Amsterdam.